Journal of Photochemistry & Photobiology A: Chemistry 393 (2020) 112414

Contents lists available at ScienceDirect

Journal of Photochemistry & Photobiology A: Chemistry

journal homepage: www.elsevier.com/locate/jphotochem

Efficient photocatalytic elimination of Temephos pesticide using ZnO nanoflowers

Amauri Serrano-Lázaro[a], Francisco A. Verdín-Betancourt[b], Vinoth Kumar Jayaraman[a], Ma. de Lourdes López-González[b], Agileo Hernández-Gordillo[a], Adolfo Sierra-Santoyo[b], Monserrat Bizarro[a,*]

[a] Instituto de Investigaciones en Materiales, Universidad Nacional Autónoma de México, Circuito Exterior S/N, Ciudad Universitaria, Coyoacán, 04510, Ciudad de Mexico, Mexico

[b] Departamento de Toxicología, Centro de Investigaciones y Estudios Avanzados del Instituto Politécnico Nacional, Av. IPN No. 2508, San Pedro Zacatenco, G.A. Madero. Ciudad de Mexico, CP 07360, Mexico

ARTICLE INFO

Keywords:
Pesticides
Temephos
Water treatment
Photocatalysis
ZnO
Nanostructures

ABSTRACT

Temephos (Tem) is a widely used pesticide to control mosquito's proliferation in tropical countries. This pesticide is put in stagnant water bodies where mosquitoes reproduce, killing larvae effectively. Recently, Tem has been identified as a DNA damaging agent; despite, people use it unmoderated in water reservoirs for personal consumption. Thus, Tem has become a hazard for human health and needs urgent attention. In order to reduce the risk of toxicity in those water sources we propose the use of nanostructured zinc oxide (ZnO) photocatalyst films to degrade this toxic compound. ZnO films with nanoflower morphology were prepared using a simple spray pyrolysis method. The band gap was 3.2 eV but a large number of natural defects present in the films allowed the absorption of visible light. The photocatalytic degradation ability of ZnO nanoflowers removed the toxic Tem under the illumination of a solar simulator. The UV–vis spectroscopy and High-Performance Liquid Chromatography analysis of Tem at regular intervals during photocatalysis confirmed the degradation of Tem, along with its transformation products or metabolites from water, reducing seven times the Tem half-life time in water. Total organic carbon measurements also indicated the mineralization of the compound.

1. Introduction

Around the world, insecticides like Scourge, Anvil, permethrin, malathion, parathion, dichlorodiphenyltrichloroethane (DDT) and temephos (Tem) are used to avoid the mosquitoes emergence [1,2], as they are vectors of harmful diseases in tropical countries [3]. There is still no successful vaccination to prevent mosquito-borne diseases such as dengue, malaria chikungunya, zika fever and West Nile virus fever [4,5]; hence controlling mosquitos' birth is an alternative to reduce these infections. Among the different pesticides, Tem was recommended by the World Health Organization as a larvicide at a concentration not exceeding 1 mg/ml [6,7]. Tem also known by its commercial name Abate [8] [4,4′-bis-(O,O-dimethyl-thionophosphoryloxy) diphenyl sulfide], is an organophosphorus insecticide used to control different flies birth such as mosquito, midge, and black fly larva over lakes, ponds, flooded areas, ditches as well as wetlands. It acts in a selective form on mosquito larvae with the inhibition of acethylcholinesterase by disrupting normal neurotransmission [9].

Tem is an unstable organophosphorus compound; its photooxidation by sunlight forms Temephos-sulfoxide (Tem-SO) and Temephos-oxon (Tem-oxon) as first metabolite products. The S-methyl isomers of Tem-SO and Tem-oxon can also take place with sunlight exposure [10,11]. Among these subproducts, Tem-SO is the most persistent one in water [12]. Recently, Benitez et al. investigated the genotoxic effect and reported that Tem caused damage in DNA of human lymphocytes even for concentrations of 1μM [13]. It has also been reported that Tem-SO metabolite could have even stronger toxicological effects than Tem [10,14,15].

The toxicological information about Tem and its metabolites is still limited and controversial [16], but clearly an adequate treatment for Tem-containing water is necessary, as the exhaustive use of Tem worldwide for several decades has resulted in the contamination of natural surface and groundwater [10]. Therefore, we propose the use of nanostructured ZnO films to treat the Tem-contaminated water by photocatalysis using sunlight, as it is a sustainable and environmentally friendly method. This method needs a semiconductor photocatalyst

* Corresponding author.
E-mail address: monserrat@iim.unam.mx (M. Bizarro).

https://doi.org/10.1016/j.jphotochem.2020.112414
Received 13 November 2019; Received in revised form 9 December 2019; Accepted 27 January 2020
Available online 30 January 2020
1010-6030/

activated by light in aerobic conditions to produce reactive oxygen species (ROS) which in turn degrade or even mineralize the organic pollutants [17,18].

The successful application of titanium dioxide to the photocatalytic degradation of pesticides has been reported [19–23]. But among the different metal oxide photocatalysts, we selected zinc oxide (ZnO) due to its excellent optical, electro-chemical and photocatalytic properties, and also for its low cost and availability. In addition, ZnO is a versatile material for which several nanostructures (nanowires, nanorods, hexagons, pyramids, flowers and needles) can be achieved as thin films by chemical or physical techniques such as pneumatic spray pyrolysis [24]. This versatile, simple and cost-effective technique allows the production of nanostructured ZnO films with nanorods or nanoflakes morphologies [25,26]. Photocatalytic ZnO films have been used to degrade several contaminant organic molecules such as dyes (methyl orange, indigo carmine, rhodamine B, malachite green, crystal violet, methylene blue etc.) [27–31], drugs (carbamazepine, paracetamol and chloramphenicol) [32,33] and other aromatic compounds such as phenolic compounds [34], but up to now, ZnO films have not yet been used for the degradation of the widely used Tem pesticide. The specific objective of this work is to provide an effective alternative for the degradation of Tem pesticide by photocatalysis using nanostructured ZnO film photocatalyst under simulated sunlight. The identification of products formed from Tem during the photocatalytic process in aerobic environment were identified by High Performance Liquid Chromatograpy (HPLC), and the mineralization percent of Tem and metabolites were determined by total organic carbon (TOC) analysis. A degradation mechanism route is established considering the formation of ˙OH radical with ZnO film.

2. Materials and methods

2.1. Synthesis and characterization of ZnO films

ZnO films were deposited by pneumatic spray pyrolysis using optimized conditions previously determined [25]. The precursor solution was prepared with 0.2 M zinc acetate dihydrate ($Zn(CH_3COO)_2{\cdot}2H_2O$, from Sigma-Aldrich > 98 %) dissolved in deionized water and few drops of acetic acid (CH_3COOH glacial from Sigma-Aldrich). Glass substrates of 2.5 × 1.25 cm were ultrasonically cleaned with trichloroethylene, acetone and methanol successively and dried with N_2 (Infra México, high pure grade). The substrates were heated at 425 °C and the previous solution was sprayed for 15 min with a gas flow rate F_g of 1028 mL/min and solution flow rate F_s of 5.3 mL/min. The nozzle was kept at a constant distance of 30 cm from the substrates.

The films were characterized by X-ray diffraction (XRD) using a Rigaku Ultima IV diffractometer with a thin film stage (Cu K_α radiation λ = 0.15418 nm). Scanning electron microscopy (SEM) images were acquired to observe the morphology with a JEOL 7600 F microscope. High-resolution transmission electron microscopy (HRTEM) images were acquired with a JEOL JEM-ARM200 F instrument. Optical transmission and absorbance spectra were measured to calculate the energy band gap E_g of the material using a Shimadzu 1800 UV–vis spectrophotometer. Photoluminescence (PL) measurements were performed on the films using a Kimmon (IK Series) He-Cd laser with a 325 nm excitation wavelength and 25 mW of power at room temperature.

2.2. Photocatalytic setup for the degradation of Temephos

Tem solution (10 mg/L) was prepared in deionized water. The solution was sonicated for 10 min before introducing the ZnO films. The film was immersed in 12 mL of Tem solution and kept in the dark for 1 h with constant stirring (1200 rpm) to achieve the adsorption-desorption equilibrium. Then, this solution with the film was irradiated with a low power sunlight simulator lamp (Oriel, 150 W, with irradiance of 360 W/m^2). An aliquot of the solution was extracted each hour and was processed as described in Section 2.3 for its further analysis by HPLC. These photocatalytic experiments and HPLC analysis were performed by triplicate (using three equivalent ZnO films). In addition, the absorption spectrum of the irradiated solution was separately recorded each hour in a Shimadzu 1800 UV–vis spectrophotometer. Total organic carbon (TOC) measurements were performed to both the control and final samples with a Shimadzu TOC-L analyzer using the high sensitivity mode. For this analysis, the NPOC method was used with the addition of HCl and bubbling with air.

2.3. Processing of Tem samples and analysis by HPLC

An aliquot was extracted from each irradiated reaction vial and transferred to the glass tubes. Then 1 ml of ammonium hydroxide (0.1 %) and 5 ml of extraction mix [8 % methanol:91 % ethyl acetate:1 % of ammonium hydroxide (0.01 %)] were added to the samples, followed by shaking in vortex for 5 min. Further, the tubes were centrifuged at 1690xg for 10 min at 4 °C. The supernatant was removed and solvent was evaporated under a gentle stream of N_2, residues were dissolved with 200 µL of methanol immediately before the analysis by HPLC as was previously reported [15]. Tem and its metabolites were analyzed using a liquid chromatograph equipped with a binary pump and a diode array detector (HPLC/DAD) (HP 1200, Agilent Technologies, Palo Alto, CA). A Zorbax Eclipse XDB column (5 µm particle size; 4.6 × 250 mm i.d.) (Deerfield, IL) was used. The retention time, recovery and precision of Temephos are shown in Table 1. The quantification of peaks was carried out by an external standard method, which included the measurement of peak areas with a five-point calibration graph. Linear relationships ($r^2 > 0.9876$) were observed in a range of 10 − 500 ng for all analytes. The identity of Tem and its metabolites (Temephos-Sulfoxide (Tem-SO), 4,4′-thiodiphenol (TDP), temephos dioxon sulfone (Tem-dox-SO_2), tempehos dioxon sulfoxide (Tem-dox-SO), 4,4′-sulfonyldiphenol (SODP), 4,4′-sulfinyldiphenol (SIDP)) was confirmed by the retention time (t_{ret}) and UV–vis spectra of standards [15].

2.4. ˙OH radical determination

The formation of ˙OH radicals in solution using ZnO films was performed by using a terephthalic acid (TA) solution at a concentration of 5 × 10^{-4} M dissolved in water/NaOH (2 × 10^{-3} M). A ZnO film was immersed in 10 mL of TA solution, left for 30 min in the dark and then irradiated with the solar simulator lamp. In the presence of ˙OH radicals, the fluorescent molecule 2-hydroxyterephthalic acid (HTA) is formed. Its fluorescence spectrum was measured using a Fluorolog3 Horiba spectrofluorometer at λ_{exc} = 350 nm.

3. Results

3.1. Characterization of ZnO films

The films showed the hexagonal wurtzite structure of ZnO (ICDD PDF No. 01-070-2551) with a preferential orientation along the c-axis as shown in Fig. 1a. The crystallite size of ZnO was 22.6 nm, obtained using Scherrer's formula. SEM images show a rough surface formed by

Table 1
Recovery and precision of Tem and its metabolites in water.

Analyte	t_{ret} (min)	Recovery (%)	Precision (%)
SIDP	3.6	106.3 ± 4.5	4.26
SODP	4.1	106.3 ± 8.6	8.07
Tem-dox-SO	5.3	101.8 ± 4.8	4.69
Tem-dox-SO_2	6.2	107.3 ± 1.2	1.07
TDP	7.7	100.8 ± 1.2	1.19
Tem-SO	10.1	98.2 ± 2.7	2.72
Tem	12.6	104.1 ± 1.2	1.11

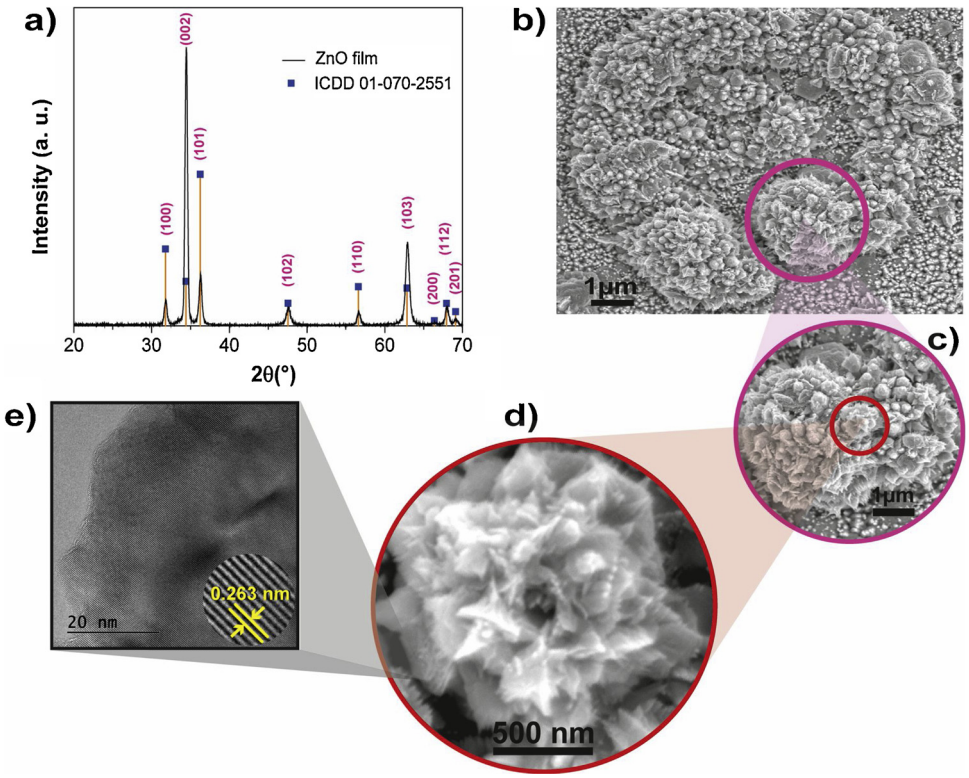

Fig. 1. (a) X-ray diffraction patterns, (b) Surface morphology observed by SEM, (c) and (d) Larger magnifications of SEM images of the ZnO thin films; e) HRTEM image of the film showing the interplanar spacing (inset).

plated nanostructures that form clusters with an aspect of "nanoflowers" with dimensions about 1.5 μm as observed in Fig. 1b, c, where the amplified image (Fig. 1d) clearly shows the "petals" of the nanoflower with dimensions of 250 nm approximately. Fig. 1e presents the HRTEM image of ZnO film, showing in the inset the interplanar spacing of the crystalline structure that was 0.263 nm, as expected for ZnO.

Optical transmission spectra were used to calculate the optical band gap (E_g), considering a direct transition. We plotted $(\alpha h\nu)^2$ *vs.* the photon energy ($h\nu$) and extrapolated the linear region to $(\alpha h\nu)^2 = 0$ (not shown) to obtain $E_g = 3.20 \pm 0.012$ eV, which is around the typical ZnO value. Fig. 2(a) depicts the absorption spectrum of ZnO film and the emission spectrum of the solar simulator used. It is observed that the absorption edge of ZnO lies in the UV portion of the solar spectrum (the inset shows an amplification of the 360 − 450 nm interval). However, it can be observed a large tail that extends to the visible region; this tail is due to the different defects present in ZnO film as corroborated by the PL shown in Fig. 2(b). The PL spectrum exhibited a small peak at 390 nm that corresponds to the near band edge transition (NBE or E_g) and a broad band centered at 503 nm, which was deconvoluted by three main contributions: one at 486 nm called blue emission, attributed to Zn^{2+} vacancies (V_{Zn}); the peak at 530 nm called green emission, originated by oxygen vacancies (V_O) and the yellow emission at 590 nm, caused by oxygen interstitials (O_i) [35]. These defects introduced several electronic states within the band gap below the conduction band, which are responsible for the absorption of photons in the visible range.

3.2. HPLC analysis of Tem solution

With the chromatographic conditions used in this study, Tem and

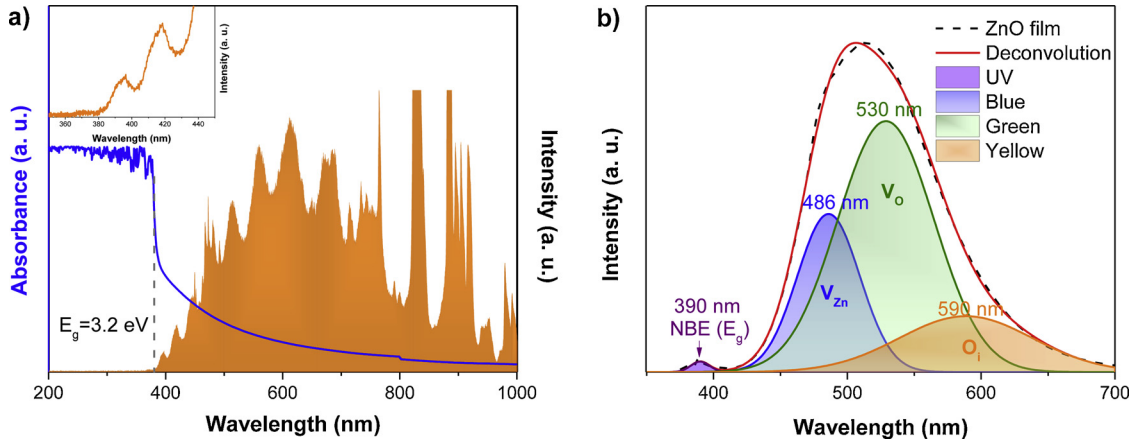

Fig. 2. (a) Absorption spectrum of ZnO film and solar simulator emission spectrum. The inset shows the UV region of the solar simulator lamp. (b) PL spectrum of ZnO film and its deconvolution to show different contributions.

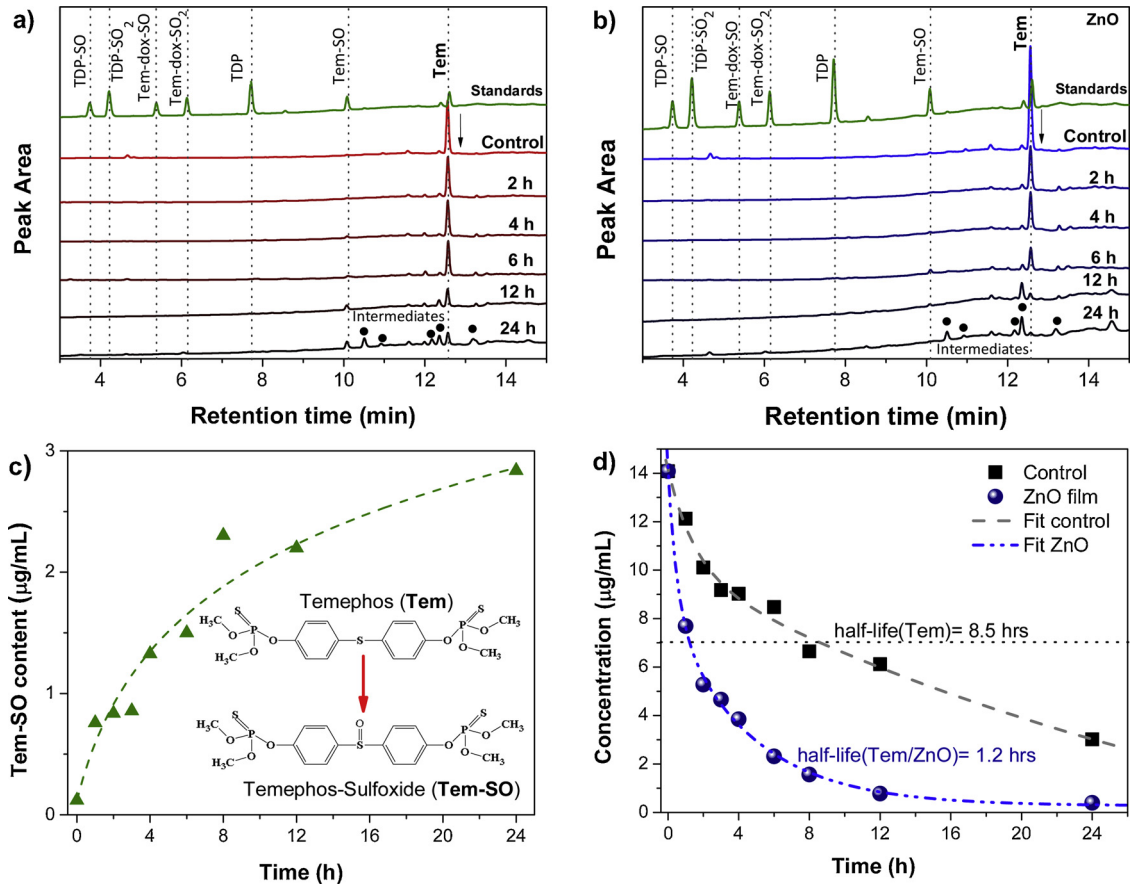

Fig. 3. HPLC Chromatogram of irradiated Tem solution in: a) absence and b) presence of ZnO film. c) Evolution of Tem-SO formation from Tem during 24 h of reaction with simulated sunlight in absence of ZnO film. d) Concentration profile from HPLC peak area of the irradiated Tem solution in absence (black) and presence (blue) of ZnO film.

six possible metabolites (transformation products) were excellently resolved within 15 min, as shown in Table 1. The quantification of peaks is the measurement of peak areas following a calibration plot. This methodology allows the identification and quantification of Tem and six of its possible metabolites in water samples. Therefore, the HPLC chromatogram of the standard used, shows the characteristic peak of Tem and its metabolites (Tem-SO, TDP, Tem-dox-SO_2, Tem-dox-SO, SODP, SIDP), as shown in Fig. 3.

Fig. 3a presents the HPLC chromatograms of irradiated Tem control solution, measured at different reaction times (2 – 24 h) without catalyst. It is clearly observed that the chromatographic peak associated to Tem, at 12.5 min slightly decreases as the reaction time progresses. After 6 h, some other small peaks were raised, suggesting the formation of new chemical species (not identified), which can be observed at retention times between 10 and 12 min. This indicates that Tem was transformed into several intermediates by the UV light action. Fig. 3b shows the HPLC chromatograms of irradiated Tem solution using ZnO film, measured after different reaction times (2 – 24 h). It is observed the diminution of Tem-peak as the reaction progresses. At 6 h of reaction the Tem-SO peak appeared; but for further reaction times, it was eliminated as well. This indicates that ZnO film is able to eliminate Tem and almost all its sub-compounds.

Fig. 3c shows the increasing concentration of Tem-SO as a result of the photo-oxidation of Tem solution while it is irradiated with simulated sunlight in the absence of ZnO. This means that during the photolysis of Tem, its principal metabolite is Tem-SO, according to previous reports [10,11]. The trend of this plot also indicates that the persistence of Tem-SO is for a long time. This is an important matter to consider because Tem-SO has stronger toxicological effects than the parent compound Tem [10,15,36,37]. However, ZnO nanostructured films demonstrated to decompose Tem, Tem-SO and other metabolites in a reasonable time under sunlight exposure. Although HPLC method can also detect other degradation products (SODP, SIDP and TDP), they were not observed. Fig. 3d shows the concentration profile of Tem obtained from the peak area of the HPLC chromatogram in the presence and absence of ZnO film. In both cases, the control sample and sample with ZnO film presented an exponential decay behavior (dashed lines) which was fitted to obtain its half-life time ($t_{1/2}$) according to the equation: $y = A_1\exp(-x/t_1)+A_2\exp(-x/t_2)$. The $t_{1/2}$ for Tem solution exposed to simulated sunlight (i.e. Tem photolysis) was 8.5 h, while for the solution in contact with the ZnO film $t_{1/2}$ reduced to only 1.2 h (indicated by the dotted line). After 12 h, Tem concentration decreased to 0.39 μg/mL, indicating almost the complete degradation of the pesticide. This is a significant result from the applied point of view, because this process can warranty the water quality of reservoirs exposed to Tem pesticide after one-day treatment with ZnO photocatalyst.

3.3. UV-absorbance of Tem solution

Fig. 4 shows the evolution of the absorption spectrum of irradiated Tem solution in the absence (a) and presence (b) of nanostructured ZnO film catalyst with sunlight exposure. The Tem solution exhibited the two characteristic absorbance bands at 257 and 285 nm. As it can be observed for the control sample, both bands were altered, exhibiting a widening with a slight decrease of absorbance. This phenomenon should be caused by the generation of metabolites (Tem-SO, TDP, Tem-dox-SO_2, Tem-dox-SO, SODP, SIDP, seen by HPLC), which present absorbance spectra in the same range as Tem contributing to the final

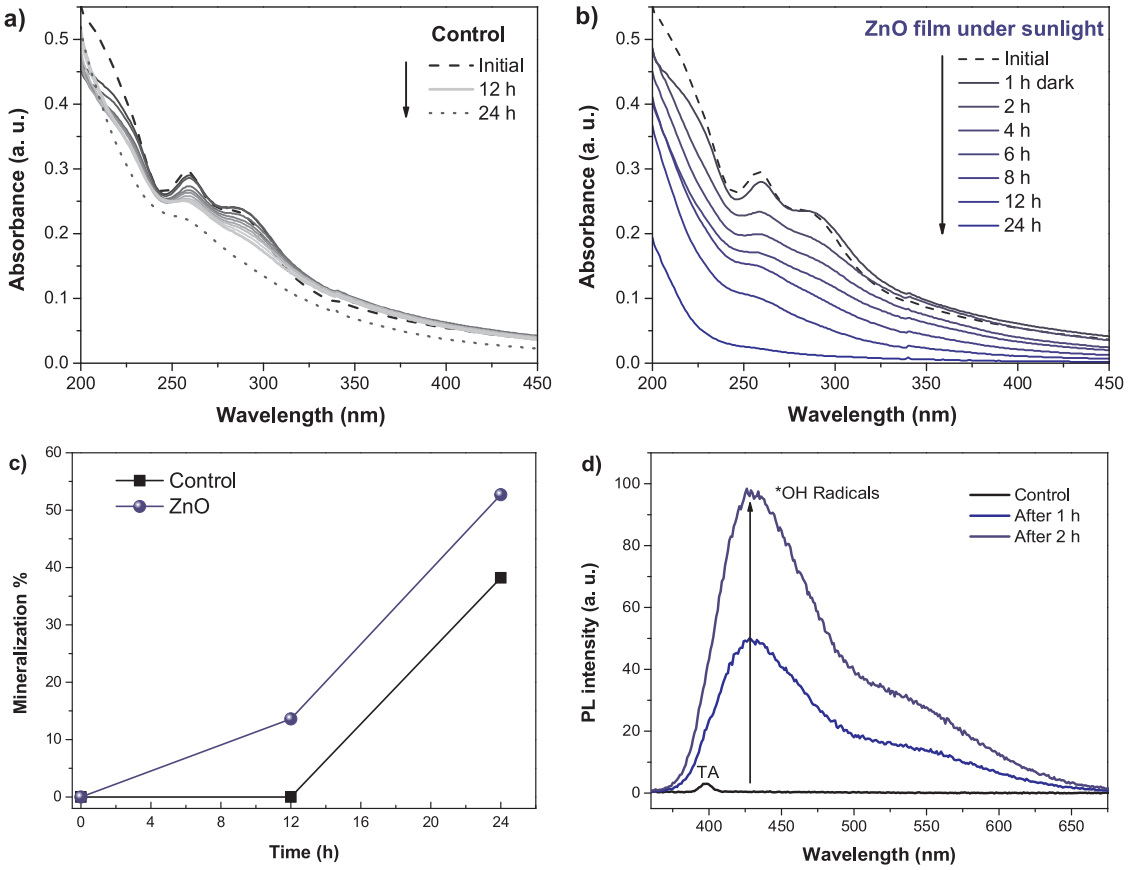

Fig. 4. UV absorption curves of Tem exposed to simulated sunlight (a) without catalyst (control sample) and (b) in the presence of ZnO film. c) Mineralization of Tem solution with and without ZnO films; d)˙OH radical determination using simulated sunlight in absence of ZnO film.

spectrum [15]. This confirms that during solar irradiation, Tem molecule suffers an alteration in its chemical structure due to the degradation process, but the concentration of Tem molecule by only UV absorbance cannot be determined as it is the superposition of the contributions of Tem and the sub-products. Whereas for the irradiated sample treated with ZnO film (Fig. 4b), the absorbance band of Tem solution continuously decreased, noticeable since the first hours. The change in the absorbance spectrum, with the inevitable band widening, suggests that few intermediates or metabolites were also generated (as was already suggested by HPLC analysis). The disappearance of the wide band suggests that Tem and all metabolites were almost degraded in 24 h. Due to the presence of some metabolites, the concentration of Tem molecule by UV absorbance cannot be determined; therefore the apparent kinetic rate constant k_{app} cannot be calculated with these data.

3.4. TOC Analysis of Tem solution and ˙OH radical

Fig. 4c presents the mineralization measured by TOC content (C^{TOC}) at the initial stage and after 12 and 24 h of simulated sunlight exposure of Tem solution. Using the equation $\%Mineralization = \% C_1^{TOC} - \% C^{TOC}$, the mineralization percent was calculated [38]. We can see that mineralization percent achieved 55 and 35 % with and without the ZnO film photocatalyst, respectively. This result suggests that the photocatalytic reaction with ZnO films effectively degrades Tem pesticide as well as part of the intermediate metabolites in comparison to the photolysis. To determine if ˙OH radicals are the reactive oxygen species responsible for the degradation process, a fluorescence test with TA was performed. When ˙OH radicals are produced at the ZnO film's surface upon irradiation, they react with TA forming HTA, which has a strong emission at 425 nm.

Fig. 4d shows the control spectrum referred to TA molecule, which has a signal at 380 nm. When ZnO film is immersed into the solution, a gradual increase in the fluorescence intensity at 425 nm, associated to the HTA formation was observed as the irradiation time increased from 1 h to 2 h. The formation of this compound confirms the generation of hydroxyl radical in presence of the ZnO film and simulated sunlight.

3.5. Stability of the photocatalytic response

The reusability of the nanoflower ZnO films was evaluated by repeating three times the degradation process with the same ZnO film. As it can be seen in Fig. 5, the performance of ZnO was almost unchanged after cycles, indicating that the material has good stability under reuses.

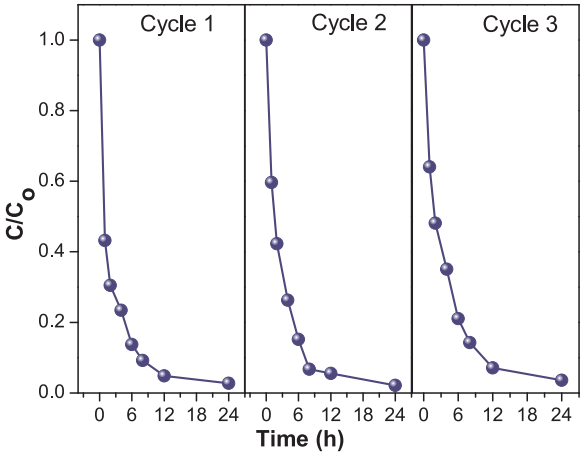

Fig. 5. Recyclability of ZnO for the degradation of Tem.

This is an important result for the further application of this material in field.

4. Discussion

Tem is an unstable organophosphorus compound widely used as larvicide, and when it is exposed to sunlight irradiation it suffers a transformation up to 80 % by photolysis after application in the field [10]. Photolysis is indeed an important way to degrade Tem and other similar pollutants [39,40] after a considerable sunlight exposure time. However, the main transformation product of Tem is Tem-SO. It is known that oxidation products of some organophosphorus pesticides (oxons, sulfoxides and sulfones) are commonly more toxic than the initial parent compound [10,15,36,37]. In this study we confirmed that indeed Tem-SO represents the main product of Tem photooxidation (Fig. 3c); therefore, it could be used as the main metabolite for monitoring water bodies since it is rapidly generated after Tem oxidation [10,12,41,42].

The effectiveness of nanostructured ZnO films in the elimination of Tem under sunlight lies in two important factors: 1) the nanostructured flower-like morphology and 2) the defects in ZnO lattice. Concerning the morphology, the flower-like structures provide high specific surface area, useful to make easy contact with Tem molecules, allowing a large number of photoactive sites available to carry out the photocatalytic reactions. Regarding the defects in ZnO crystalline structure, PL curves revealed a large number of defects within ZnO's band gap. The deconvolution analysis of the broad band in the visible region (Fig. 2b) shows a very large contribution of oxygen vacancies (green emission at 530 nm), but also Zn vacancies (blue emission at 486 nm) and oxygen interstitials (yellow emission at 590 nm). All these defects are localized states within the band gap allowing the absorption of a large amount visible light photons, that make ZnO highly effective under sunlight. These defects also act as electron traps, leading the separation of the charge carrier pairs and allowing the generation of great amount of reactive oxygen species. Due to that we demonstrated that ZnO flower-like morphology favors the production of $^{\cdot}OH$ radicals, in concordance with the previously reported [25], which are the active species responsible for the degradation of Tem.

The proposed photocatalytic mechanism for the fast degradation of Tem and its metabolites is described in the following equations:

$$ZnO + h\nu \rightarrow e^{-} + h^{+}$$

$$h^{+} + H_2O \rightarrow {}^{\cdot}OH + H^{+}$$

$$^{\cdot}OH + \text{Tem} \rightarrow \text{Tem-SO}$$

$$^{\cdot}OH + \text{Tem-SO} \rightarrow \text{Tem-fragments} + \text{mineralization}$$

When a photon with energy $h\nu$ excites ZnO semiconductor, the electron-hole pairs are photogenerated and both migrate to the film surface. Then, the hole, h^{+}, interacts with a water molecule to form the hydroxyl radical. This highly reactive species reacts with the Tem molecule and easily oxidizes to Tem-SO. This formed Tem-SO again interacts with another hydroxyl radical to continue the degradation of the molecule into other Tem-fragments. Simultaneously, the separated electron e^{-} interacts with the dissolved oxygen present into solution to produce at the end more hydroxyl radicals, which in turn, mineralize the Tem-fragments into inorganic molecules. Thus, flower-like ZnO films can be potentially applied *in situ* to degrade Tem-polluted water under natural sunlight irradiation.

5. Conclusions

This study demonstrates that flower-like nanostructured ZnO films with crystal defects produced by spray pyrolysis efficiently generate the hydroxyl radicals to degrade Tem pesticide in water while exposed to simulated sunlight irradiation. Tem-metabolites (such as Tem-SO, the most persistent one) were the main degradation-products and were also effectively mineralized (about 50 % in 24 h), as all their corresponding HPLC signals were under the limit of detection after 24 h of reaction. Moreover, ZnO films decreased the $t_{1/2}$ of Tem from 8.5 h to only 1.2 h, i.e. the use of ZnO makes the reaction more efficient by 7 times in comparison to the photolysis. The proposed mechanism indicates that the degradation process occurs via $^{\cdot}OH$ radicals which effectively attack both Tem and Tem-SO molecules until their complete mineralization. This makes nanostructured ZnO films a suitable material for the photocatalytic treatment of water containing Tem pesticide.

CRediT authorship contribution statement

Amauri Serrano-Lázaro: Investigation, Formal analysis, Data curation, Visualization. **Francisco A. Verdín-Betancourt:** Methodology, Validation, Investigation. **Vinoth Kumar Jayaraman:** Investigation, Formal analysis, Writing - original draft. **Ma. de Lourdes López-González:** Resources. **Agileo Hernández-Gordillo:** Writing - review & editing. **Adolfo Sierra-Santoyo:** Conceptualization, Methodology, Supervision, Project administration, Writing - review & editing. **Monserrat Bizarro:** Conceptualization, Supervision, Formal analysis, Writing - original draft, Writing - review & editing, Project administration, Funding acquisition.

Declaration of Competing Interest

None.

Acknowledgements

The authors thank Omar Novelo, Josué Romero, Carlos Ramos, Adriana Tejeda for the technical support during the characterization of the films. This project was financially supported by UNAM-PAPIITIN108618.

Appendix A. Supplementary data

Supplementary material related to this article can be found, in the online version, at doi:https://doi.org/10.1016/j.jphotochem.2020.112414.

References

[1] M. Vijayaraghavan, B. Nagarajan, Mutagenic potential of acute exposure to organophosphorus and organochlorine compounds, Mutat. Res. Toxicol. 321 (1994) 103–111.
[2] D. Goindin, C. Delannay, A. Gelasse, C. Ramdini, T. Gaude, F. Faucon, J.P. David, J. Gustave, A. Vega-Rua, F. Fouque, Levels of insecticide resistance to deltamethrin, malathion, and temephos, and associated mechanisms in Aedes Aegypti mosquitoes from the Guadeloupe and Saint Martin Islands (French West Indies), Infect. Dis. Poverty 6 (2017) 1–15.
[3] A.I. Qureshi, A.I. Qureshi (Ed.), Mosquito-Borne Diseases, Academic Press, 2018, pp. 27–45.
[4] C.M. Anderson, A world without sanctuary, Fam. Process 41 (2002) 1–3.
[5] S.N. Tikar, A. Kumar, G.B.K.S. Prasad, S. Prakash, Temephos-induced resistance in Aedes aegypti and its cross-resistance studies to certain insecticides from India, Parasitol. Res. 105 (2009) 57–63.
[6] J.A. Rozendaal, Vector Control, Methods for Use by Individuals and Communities, World Health Organization, Geneva, 1997, p. 424.
[7] D.C. Chavasse, H.H. Yap, Chemical Methods for the Control of Vectors and Pests of Public Heath Importance, World Health Organization, 1997 129 p..
[8] M. Velki, S. Stepić, B.K. Hackenberger, Effects of Formalin on some biomarker activities of earthworms pre-exposed to temephos, Chemosphere 90 (2013) 2690–2696.
[9] A. Ferguson, J.B. Taggart, P.A. Prodöhl, O. McMeel, C. Thompson, C. Stone, P. McGinnity, R.A. Hynes, The application of molecular markers to the study and conservation of fish populations, with special reference to Salmo, J. Fish Biol. 47 (1995) 103–126.
[10] S. Lacorte, N. Ehresmann, D. Barceló, Persistence of temephos and its transformation products in rice crop field waters, Environ. Sci. Technol. 30 (1996) 917–923.
[11] J.P.G. Wilkins, Rationalisation of the mass spectrometric and gas chromatographic behaviour of organophosphorus pesticides: part 1–substituted phenyl

phosphorothioates, Pestic. Sci. 29 (1990) 163–181.
[12] S. Lacorte, D. Barceló, Determination of organophosphorus pesticides and their transformation products in river waters by automated on-line solid-phase extraction followed by thermospray liquid chromatography-mass spectrometry, J. Chromatogr. A 712 (1995) 103–112.
[13] A.B. Benitez-Trinidad, J.F. Herrera-Moreno, G. Vázquez-Estrada, F.A. Verdín-Betancourt, M. Sordo, P. Ostrosky-Wegman, Y.Y. Bernal-Hernández, I.M. Medina-Díaz, B.S. Barrón-Vivanco, M.L. Robledo-Marenco, Cytostatic and genotoxic effect of temephos in human lymphocytes and HepG2 cells, Toxicol. In Vitro 29 (2015) 779–786.
[14] M. Jokanovic, Biotransformation of organophosphorus compoun, Toxicology 166 (2001) 22.
[15] F.A. Verdín-Betancourt, M. Figueroa, Md.L. López-González, E. Gómez, Y.Y. Bernal-Hernández, A.E. Rojas-García, A. Sierra-Santoyo, *In vitro* inhibition of human red blood cell acetylcholinesterase (AChE) by temephos-oxidized products, Sci. Rep. 9 (2019) 14758.
[16] W. Renshaw, A. Bobbis, Temephos. En: Joint by FAO and WHO, with the support of the International Programme on Chemical Safety/Joint Meeting of the FAO Panel of Experts on Pesticide Residues in Food and the Environment and WHO Core Assessment Group. Pesticide Residues in Food. T, (2006).
[17] J.M. Herrmann, Heterogeneous photocatalysis: state of the art and present applications In honor of Pr. R.L. Burwell Jr. (1912–2003), Former Head of Ipatieff Laboratories, Northwestern University, Evanston (Ill), Top Catal 34 (2005) 49–65.
[18] A. Syed Nabeel, H. Waseem, Heterogeneous photocatalysis and its potential applications in water and wastewater treatment: a review, Nanotechnology 29 (2018) 342001.
[19] M. Abdennouri, M. Baâlala, A. Galadi, M. El Makhfouk, M. Bensitel, K. Nohair, M. Sadiq, A. Boussaoud, N. Barka, Photocatalytic degradation of pesticides by titanium dioxide and titanium pillared purified clays, Arab. J. Chem. 9 (2016) S313–S318.
[20] R. Fiorenza, A. Di Mauro, M. Cantarella, C. Iaria, E.M. Scalisi, M.V. Brundo, A. Gulino, L. Spitaleri, G. Nicotra, S. Dattilo, S.C. Carroccio, V. Privitera, G. Impellizzeri, Preferential removal of pesticides from water by molecular imprinting on TiO2 photocatalysts, Chem. Eng. J. 379 (2020) 122309.
[21] R. Fiorenza, A. Di Mauro, M. Cantarella, V. Privitera, G. Impellizzeri, Selective photodegradation of 2,4-D pesticide from water by molecularly imprinted TiO2, J. Photochem. Photobiol. A: Chem. 380 (2019) 111872.
[22] C.B.D. Marien, T. Cottineau, D. Robert, P. Drogui, TiO2 nanotube arrays: influence of tube length on the photocatalytic degradation of paraquat, Appl. Catal. B Environ. 194 (2016) 1–6.
[23] H. Hossaini, G. Moussavi, M. Farrokhi, The investigation of the LED-activated FeFNS-TiO2 nanocatalyst for photocatalytic degradation and mineralization of organophosphate pesticides in water, Water Res. 59 (2014) 130–144.
[24] Z.L. Wang, Nanostructures of zinc oxide, Mater. Today 7 (2004) 26–33.
[25] V.K. Jayaraman, A. Hernández-Gordillo, M. Bizarro, Importance of precursor type in fabricating ZnO thin films for photocatalytic applications, Mater. Sci. Semicond. Process. 75 (2018) 36–42.
[26] N.S. Portillo-Vélez, M. Bizarro, Sprayed pyrolyzed ZnO films with nanoflake and nanorod morphologies and their photocatalytic activity, J. Nanomater. 2016 (2016) 11.
[27] L.A. Ghule, A.A. Patil, K.B. Sapnar, S.D. Dhole, K.M. Garadkar, Photocatalytic degradation of methyl orange using ZnO nanorods, Toxicol. Environ. Chem. 93 (2011) 623–634.
[28] N.S. Portillo-Vélez, A. Hernéndez-Gordillo, M. Bizarro, Morphological effect of ZnO nanoflakes and nanobars on the photocatalytic dye degradation, Catal. Today 287 (2017) 106–112.
[29] N. Kaneva, I. Stambolova, V. Blaskov, Y. Dimitriev, S. Vassilev, C. Dushkin, Photocatalytic activity of nanostructured ZnO films prepared by two different methods for the photoinitiated decolorization of malachite green, J. Alloys Compd. 500 (2010) 252–258.
[30] S.B. Ameur, H. Belhadjltaief, A. Barhoumi, B. Duponchel, G. Leroy, M. Amlouk, H. Guermazi, Physical investigations and photocatalytic activities on ZnO and SnO_2 thin films deposited on flexible polymer substrate, Vacuum 155 (2018) 546–552.
[31] X. Xue, W. Zang, P. Deng, Q. Wang, L. Xing, Y. Zhang, Z.L. Wang, Piezo-potential enhanced photocatalytic degradation of organic dye using ZnO nanowires, Nano Energy 13 (2015) 414–422.
[32] D.P. Mohapatra, S.K. Brar, R. Daghrir, R.D. Tyagi, P. Picard, R.Y. Surampalli, P. Drogui, Photocatalytic degradation of carbamazepine in wastewater by using a new class of whey-stabilized nanocrystalline TiO2 and ZnO, Sci. Total Environ. 485–486 (2014) 263–269.
[33] I.A. Pronin, N.V. Kaneva, A.S. Bozhinova, I.A. Averin, K.I. Papazova, D.T. Dimitrov, V.A. Moshnikov, Photocatalytic oxidation of pharmaceuticals on thin nanostructured zinc oxide films, React. Kinet. Catal. Lett. 55 (2014) 167–171.
[34] H. Benhebal, M. Chaib, T. Salmon, J. Geens, A. Leonard, S.D. Lambert, M. Crine, B. Heinrichs, Photocatalytic degradation of phenol and benzoic acid using zinc oxide powders prepared by the sol-gel process, Alexandria Eng. J 52 (2013) 517–523.
[35] N.H. Alvi, K. ul Hasan, O. Nur, M. Willander, The origin of the red emission in n-ZnO nanotubes/p-GaN white light emitting diodes, Nanoscale Res. Lett. 6 (2011) 130.
[36] M. Jokanović, Biotransformation of organophosphorus compounds, Toxicology 166 (2001) 139–160.
[37] Y.A. Kim, H.S. Lee, Y.C. Park, Y.T. Lee, A convenient method for oxidation of organophosphorus pesticides in organic solvents, Environ. Res. 84 (2000) 303–309.
[38] A. Hernández-Gordillo, M. Bizarro, T.A. Gadhi, A. Martínez, A. Tagliaferro, S.E. Rodil, Good practices for reporting the photocatalytic evaluation of a visible-light active semiconductor: Bi2O3, a case study, Catal. Sci. Technol. 9 (2019) 1476–1496.
[39] W.M.C. Draper, D. G, Solar photooxidation of pesticides in dilute hydrogen peroxide, J. Agric. Food Chem. 32 (1984) 231–237.
[40] H.B. Wan, M.K. Wong, C.Y. Mok, Comparative study on the quantum yields of direct photolysis of organophosphorus pesticides in aqueous solution, J. Agric. Food Chem. 42 (1994) 2625–2630.
[41] A. Kamel, C. Byrne, C. Vigo, J. Ferrario, C. Stafford, G. Verdin, F. Siegelman, S. Knizner, J. Hetrick, Oxidation of selected organophosphate pesticides during chlorination of simulated drinking water, Water Res. 43 (2009) 522–534.
[42] S. Lacorte, G. Jeanty, J.L. Marty, D. Barcelo, Identification of fenthion and temephos and their transformation products in water by high-performance liquid chromatography with diode array detection and atmospheric pressure chemical ionization mass spectrometric detection, J. Chromatogr. A 777 (1997) 99–114.